

Original article

Synthesis, characterization and antimicrobial activity of Fe(II), Zn(II), Cd(II) and Hg(II) complexes with 2,6-bis(benzimidazol-2-yl)pyridine ligand

Naz M. Aghatabay^{a,*}, A. Neshat^b, T. Karabiyik^a, M. Somer^c, D. Hacıu^c, B. Dülger^d

^a Department of Chemistry, Fatih University, Büyükcemece, 34500 Istanbul, Turkey

^b Department of Chemistry, MS 602, University of Toledo, Toledo, OH 43606, USA

^c Department of Chemistry, Koç University, Rumelifeneri Yolu, Sariyer, 34450 Istanbul, Turkey

^d Department of Biology, Canakkale Onsekiz Mart University, Canakkale, Turkey

Received 9 February 2006; received in revised form 28 July 2006; accepted 28 September 2006

Available online 26 December 2006

Abstract

2,6-Bis(benzimidazol-2-yl)pyridine (L) ligand and complexes $[M(L)Cl_2]$ and $[Fe(L)_2](ClO_4)_2$ ($M = Zn, Cd, Hg$) have been synthesized. The geometries of the $[M(L)Cl_2]$ complexes were derived from theoretical calculation in DGauss/DFT level (DZVP basis set) on CACHE. The central M(II) ion is penta-coordinated and surrounded by N_3Cl_2 environment, adopting a distorted trigonal bipyramidal geometry. The ligand is tridentate, *via* three nitrogen atoms to metal centre and two chloride ions lie on each side of the distorted benzimidazole ring. In the $[Fe(L)_2](ClO_4)_2$ complex, the central Fe(II) ion is surrounded by two (3N) units, adopting an octahedral geometry. The elemental analysis, molecular conductivity, FT-Raman, FT-IR (mid-, far-IR), 1H , and ^{13}C NMR were reported. The antimicrobial activities of the free ligand, its hydrochloride salt, and the complexes were evaluated using the disk diffusion method in dimethyl sulfoxide (DMSO) as well as the minimal inhibitory concentration (MIC) dilution method, against 10 bacteria and the results compared with that for gentamycin. Antifungal activities were reported for *Candida albicans*, *Kluyveromyces fragilis*, *Rhodotorula rubra*, *Debaryomyces hansenii*, *Hanseniaspora guilliermondii*, and the results were referenced against nystatin, ketoconazole, and clotrimazole antifungal agents. In most cases, the compounds tested showed broad-spectrum (Gram positive and Gram negative bacteria) activities that were either more effective than or as potent as the references. The binding of two most biologically effective compounds of zinc and mercury to calf thymus DNA has also been investigated by absorption spectra.

© 2006 Elsevier Masson SAS. All rights reserved.

Keywords: Antifungal; Antimicrobial; Equipotent; Metabolites; Tridentate; Trigonal bipyramidal

1. Introduction

Since the use of cisplatin – $[Pt(NH_3)_2Cl_2]$ as an effective anticancer drug, the interest toward transition metal complexes containing N-donor ligands has increased in order to obtain metal-based drugs exhibiting a high biological activity together with a reduced toxicity [1–3]. In this respect, benzimidazole derivatives together with their transition metal

complexes have been extensively investigated [4–6]. One of the most attractive features of these ligands in the field of biological investigation has been their structural similarities with the common pyrimidine and purine type nucleobases. In the imidazole class, nucleosides of amino derivatives are biologically active site, while in the bisbenzimidazole class it is nucleosides of the ring substitutions and bridging sections that are becoming well known bioactive site [7–9]. The interaction of metal ions with biologically active ligands, for instance in drugs, is a subject of great interest. Some of the biologically active complexes do act *via* chelation or according to preferences dictated by the hard–soft theory of acids and bases,

* Corresponding author. Tel.: +90 212 8663300; fax: +90 212 8663402.

E-mail address: natabay@fatih.edu.tr (N.M. Aghatabay).

but for most, little is known about how metal coordination influences their activity [10–12]. The most successful compounds seem to be those that interfere with the construction of the bacterial cell wall, the process of protein synthesis, and replication or transcription of DNA. In this respect, the metal oxidation state, the type and the number of donor atoms, as well as their relative disposition within the ligand are major factors determining structure–activity relationship of metal complexes. These studies are also important for the probes of nucleic acid structure and in determining the mechanism of metal ion toxicity. There has been substantial interest in understanding the binding properties of metal complexes, with biomolecules such as nucleic acids, proteins and lipids [13].

As borderline elements the iron(II) and zinc(II) are the most abundant ubiquitous and essential trace elements in biological system they serve more biological roles than any other metal ions. They have been identified as catalytic components of many enzymes and play several vital structural roles in a large number of proteins, transportations and transcription factors. Their binding properties with the biomolecules, particularly to the oxygen and nitrogen donor centres, serve their bio-functionality. On the other hand, nonessential cadmium(II) and mercury(II) are very soft acids with very high toxicity. Their salts have a long history of use as antibacterial agents. One of the best illustrations of these metal ions principle in biochemistry is provided by the metallothionein. Metallothionein is a generic name for a super family of ubiquitous low molecular weight metalloproteins possessing a unique type of sulphur-based metal cluster. Vital roles for this pleiotropic protein result in its involvement in homoeostasis of essential trace metals such as zinc, or sequestration of the environmental toxic metals namely cadmium and mercury. Herein, we describe the structural, biological activity and DNA binding properties of this very important planar tridentate ligand and its transition metal complexes. Only few information has been reported for the $[\text{Fe}(\text{L})_2](\text{ClO}_4)_2$ and $[\text{Cd}(\text{L})\text{Cl}_2]$ complexes lacking any detailed spectroscopic study or biological investigation [14–16].

2. Chemistry

Ligand (L) is prepared by literature procedures [5,17]. Syntheses of the complexes are carried under reflux in EtOH. Full

general procedures for the preparation of these compounds are given in Section 6. The spectroscopic data from the FT-Raman, FT-IR, ^1H and ^{13}C NMR together with molar conductivity measurements do provide useful information for their formation and structural characterization. Optimized structures of the ligand and $[\text{Zn}(\text{L})\text{Cl}_2]$ complex are presented in Figs. 1 and 2. Required analytical data and physical properties are summarized in Table 1.

3. Theoretical calculation

The structure of the ligand and the $[\text{Zn}(\text{L})\text{Cl}_2]$ complex was refined by performing a geometry optimization calculation in DGauss/DFT (density functional theory) available on CACHE work system pro version 6.1.10 package program. The B88-PW91 with the widely-used DZVP basis set, uses Beck's [18] exchange functional and Perdew's [19] correlation functional of the generalized gradient approximation (GGA). The theoretical calculation of the off-resonance ^{13}C NMR spectrum of the ligand was carried out using NMR simulation gNMR 4.1 program at version level 4.1.

4. Biological data

Gentamycin inhibits protein synthesis by binding to ribosomal subunit, nystatin works by binding to sterols in the fungal cellular membrane altering the permeability to allow leakage of the cellular contents and destroying the fungus, ketoconazole inhibits the growth of fungal organisms by interfering with the formation of the fungal cell wall and clotrimazole kills fungi and yeasts by interfering with their cell membranes and causing essential constituents of the fungal cells leakage. Mueller–Hinton media, nutrient broth and malt extract broth are purchased from Difco and yeast extracts are obtained from Oxoid.

5. Results and discussions

5.1. Chemistry

5.1.1. Nuclear magnetic resonance

^1H and ^{13}C spectral data of the free ligand and $[\text{M}(\text{L})\text{Cl}_2]$ ($\text{M} = \text{Zn}, \text{Cd}, \text{Hg}$) are presented in Table 2. The ^1H NMR

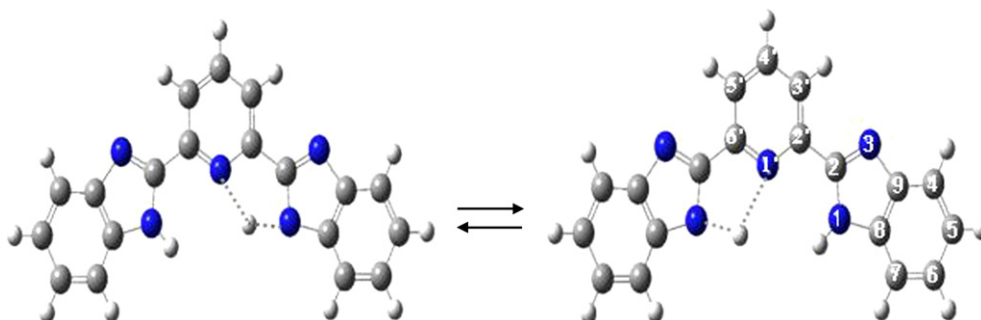


Fig. 1. Structure of the ligand (L).

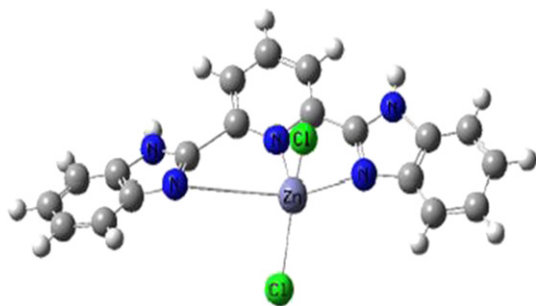


Fig. 2. Structure of the $[Zn(L)Cl_2]$ complex.

spectrum of the ligand exhibits a singlet at 13.1 ppm owing to the imine proton atom N–H. The resonances corresponding to the two equivalent benzimidazole groups are located at 7.33_t, 7.40_t, 7.79_d and 7.84_d ppm. In addition the pyridine moiety displays two signals, a triplet at 8.22 and a doublet at 8.38 ppm due to the (1H-4', t) and (2H-3', 5', d) protons. Apart from imine proton atoms, all the other proton signals are also observed at nearly identical positions in the complexes bearing different coupling patterns compared with the free ligand. However, the signal due to N–H proton in the mercury complex is observed as a broad band in the 13–10 ppm region, while the signals for the other complexes are not observed. These protons either resonate along with aromatic protons or may appear beyond 15 ppm [20].

The ^{13}C NMR spectrum of the benzimidazole moiety in the ligand, exhibits six signals for the benzene ring carbon atoms. The nitrogen atom of pyridine unit is capable to form intramolecular hydrogen bonding with N–H group of benzimidazole moiety resulting the inhibition of fluxional behaviour of N₁–H–N₃ unit (Fig. 1), creating an asymmetric *o*-substituted molecule and therefore as expected the ^{13}C spectrum of the uncoordinated ligand exhibits 10 signals in the range 112.12–150.82 ppm (Table 2). The assignments of the signals are made with the aid of theoretical calculation of the off-resonance ^{13}C spectrum of the ligand and as well as in comparison with the reported values [21].

The spectral pattern will change in the complex due to the coordination with lowering of the electron density in the ligand system, resulting possible downfield chemical shifts of the carbon signals. Significant chemical shifts are observed for C-2, 150.82 → 165.94; C-9, 144.50 → 148.15; C-8, 134.07 → 147.36 in the $[Hg(L)Cl_2]$ complex. Similar shifts are also observed for the $[Cd(L)Cl_2]$ and $[Zn(L)Cl_2]$

complexes. These strong downfield resonances on these carbon atoms are most probably caused by de-shielding effect of the nitrogen atoms, which tend to support coordination via nitrogen atoms (Table 2).

5.1.2. Infrared and Raman spectra

The prominent vibrational spectral data for free ligand and the $[M(L)Cl_2]$ complexes together with their assignments are presented in Table 3 and the spectra are shown in Figs. 3–7. The N–H stretching and bending vibrations of the ligand at 3193 and 1460 cm^{-1} , remain either unperturbed or undergo a slight shift in the complexes, suggesting that the imine proton remains attached at the N-1 position. The broadness of the stretching vibration is very likely the result of the intramolecular hydrogen bonding. These modes didn't appear in the Raman spectra, due to their weak intensity. The pure characteristic $\nu(C-H)$ modes of the ring residues are observed as expected in the wave regions 3100 cm^{-1} both in IR and Raman spectra. Slight but specific differences between the spectra of the free ligand and the coordination compounds in this region point to the formation of new complexes. The presence of a sharp medium band at 1602 cm^{-1} in IR spectrum and weak band at 1625 cm^{-1} in Raman spectrum, owing to $\nu(C-C)$ (ring) vibration in the free ligand shifts to higher frequency at ca. 1628 cm^{-1} . The appearance of sharp strong bands at ~ 1600 cm^{-1} in both IR and Raman spectra, owing to the $\nu_{as}(C=N)$ (imine moiety) vibrations in the complexes, indicate the bonding of imine nitrogen atoms with the metal ions. Such vibration in the free ligand appears as a weaker band at 1589 cm^{-1} . The comparison of bands for $\nu_{as}(C-N)$ (pyridine moiety) vibrations of the ligand and complexes is somewhat difficult owing to appearance of this band along with bands of the nitrogen of the benzimidazole residue. However, presence of strong bands at ~ 1580 cm^{-1} in Raman and at ~ 1590 cm^{-1} in IR spectra in the complexes could represent the respective $\nu_{as}(C-N)$ stretches.

On complexation, very strong band appears at ~ 1450 cm^{-1} both in Raman and IR and are interpreted as $\nu_s(C=N)$ frequencies of the coordinated ligand, through its imine nitrogen atoms. However, this mode is not characteristic and is strongly coupled with several other vibrations, including $\nu(C-H)$, $\nu(N-H)$ and $\nu(C-C)$ (Table 3, Figs. 3 and 4).

Of particular interest is the lower frequency region, characteristic for the metal–chloride and metal–nitrogen stretching vibrations. The Raman spectra of the anhydrous solid metal

Table 1
The analytical data and physical properties of the ligand and complexes

Compound	Found (calculated)			Colour	Yield %	M.p./dec	Δm
	C	H	N				
$C_{19}H_{13}N_5$ (L)	—	—	—	White	75	195	—
$ZnC_{19}H_{13}N_5Cl_2$ [A]	51.0 (49.7)	2.9 (3.1)	15.7 (15.3)	P-y	68	>300	6.1
$CdC_{19}H_{13}N_5Cl_2$ [B]	46.1 (45.3)	2.6 (2.8)	14.2 (13.9)	White	63	>300	5.7
$HgC_{19}H_{13}N_5Cl_2$ [C]	39.1 (38.7)	2.2 (2.4)	12.0 (11.7)	White	65	>300	7.8
$[Fe(L)_2](ClO_4)_2$ [D]	—	—	—	R-b	70	>320	—

Δm , Molar conductivity $\Omega^{-1} cm^2 mol^{-1}$; r-b, reddish-brown; p-y, pale-yellow; dec, decompose.

Table 2
¹H chemical shifts (ppm) for the ligand (L) and complexes

Compound	4 (2H)	5 (2H)	6 (2H)	7 (2H)	NH (2H)	3' (1H)	4' (1H)	5' (1H)
L	7.79, 7.84m	7.4m, 7.33m	7.4, 7.33m	7.79, 7.74m	13.1s	8.38d	8.22t	8.38d
[A]	7.84m, 7.72m	7.44m, 7.32m	7.44m, 7.32m	7.84m, 7.72m		8.6–8.2m	8.6–8.2m	8.6–8.2m
[B]	7.88m, 7.76m	7.48m, 7.35m	7.48m, 7.35m	7.88m, 7.76m		8.6–8.2m	8.6–8.2m	8.6–8.2m
[C]	7.82m, 7.72m	7.45m, 7.23m	7.45, 7.23m	7.8m, 7.72m	13–10	8.5–8.25m	8.5–8.25m	8.5–8.25m

Observed and theoretical ¹³C chemical shifts (ppm) for the ligand (L) and complexes

Comp.	2	4	5	6	7	8	9	2'	3'	4'	5'	6'
(L) ^a	150.82	120.06	124.08	122.55	112.12	134.07	144.5	148.08	121.71	139.55	121.71	148.08
(L) ^b	150.13	116.65	123.48	123.25	116.11	138.89	140.08	150.88	117.68	138.84	117.68	150.88
[A]	165.51	122.95	125.91	124.99	116.6	147.9	148.2	149.46	124.57	138.42	124.57	149.46
[B]	165.54	123.19	125.69	124.5	115.89	148.1	149.45	149.6	124.27	141.11	124.27	149.6
[C]	165.94	124.52	126.44	125.77	123.3	147.36	148.15	149.98	124.88	140.92	124.88	149.98

^a Experimental data.

^b Theoretical data.

halides M–Cl (Hg, Cd, Zn) are illustrated in Fig 5. The most intense bands appearing at 314 (Hg), 229 (Zn) and 221 cm⁻¹ (Cd) represent the $\nu(\text{metal–Cl})$ vibration frequencies. However, the position of the four-fold coordinating chloride atoms in these salts is only bridging while in the title compounds both (metal–Cl) bonds are terminal. Therefore, the values of the (metal–Cl) stretches taken from the tetrahedral [M(pyridine)₂Cl₂] complex series are more helpful for comparison. These vibrations have been located in 350–250 cm⁻¹ region [22,23]. The two metal–chloride bonds in the [M(L)Cl₂] complexes give rise to a pair of bands in both IR and Raman spectra which are interpreted as $\nu_{\text{as}}(\text{M–Cl})$ and $\nu_{\text{s}}(\text{M–Cl})$ vibrations (Table 3, Figs. 6 and 7).

Based on the vibrational spectroscopic data for the different Zn–pyridine [23–25] both the antisymmetric and symmetric vibrations of metal–nitrogen stretches are expected to appear

in 250–180 cm⁻¹ region. However, in the title compounds the nitrogen ligands are not “free” but integrated in a chelate ring (Fig. 2). The bands at 203, 179 in the IR and 205, 192 cm⁻¹ in the Raman spectra for the [Hg(L)Cl₂] complex may be assignable to these two vibration modes, respectively. Similar values are expected also for the [Cd(L)Cl₂] and [Zn(L)Cl₂] complexes, since the effect of the metal ions will be small on metal–nitrogen stretching vibrations (Table 3).

5.1.3. Electronic spectra

The [Zn(L)Cl₂] and [Hg(L)Cl₂] complexes show absorbance at 315 and 312 nm, respectively, which may be assignable to $n \rightarrow \pi^*$ and $\pi \rightarrow \pi^*$ ligand field transitions. Nitrogen \rightarrow metal charge transfer for zinc complex is observed as shoulders at 346 and 366 nm, whereas for the mercury complex the same transitions occur at 324 and 350 nm

Table 3
 Prominent IR (mid and far) and Raman bands for the ligand Bzp and complexes

Compound	FT-IR (cm ⁻¹)	Raman (cm ⁻¹)
(L)	3193vs $\nu(\text{N–H})$, 3063s $\nu(\text{C–H})$, 1602m $\nu(\text{C–C})$, 1589m $\nu_{\text{as}}(\text{C–N})$, 1574s, 1460vs [$\nu_{\text{s}}(\text{C–N})$, $\delta(\text{N–H})$, $\nu(\text{C–H})$], 1435vs, 1317vs, 1278vs [$\nu(\text{C–N})$, $\nu(\text{C–C})$], 1231m, 820s, 742vs, 694m, 451m, 419s, 402s, 350s, 322m, 287s, 277sh, 217m, 174m.	3075m $\nu(\text{C–H})$, 1625w $\nu(\text{C–C})$, 1596s $\nu(\text{C–N})$, 1575vs, 1538s, 1455s [$\nu_{\text{s}}(\text{C–N})$, $\delta(\text{N–H})$, $\nu(\text{C–H})$], 1282s, 1267s [$\nu_{\text{s}}(\text{C–N})$, $\nu(\text{C–C})$], 1008w, 996s, 870w, 804w, 651w, 626w, 291w, 196m.
[A]	3442m $\nu(\text{H–O–H})$, 3180s $\nu(\text{N–H})$, 3100 $\nu(\text{C–H})$, 1629m $\nu(\text{C–C})$, 1608 $\nu(\text{C–N})$, 1589s, 1495s, 1482s, 1460vs [$\nu_{\text{s}}(\text{C–N})$, $\delta(\text{N–H})$, $\nu(\text{C–H})$], 1427s, 1317vs, 1147m, 820s, 744vs, 666m, 583m, 488s, 432s, 397m, 332s, 289s, 269mb, 221m.	3073m $\nu(\text{C–H})$, 1630s $\nu(\text{C–C})$, 1611sn $\nu(\text{C–N})$, 1579s, 1554s, 1539vs, 1447vs [$\nu_{\text{s}}(\text{C–N})$, $\delta(\text{N–H})$, $\nu(\text{C–H})$], 1267vs [$\nu(\text{C–N})$, $\nu(\text{C–C})$], 1154m, 1017s, 973m, 808w, 585m, 533s, 333s, 316m $\nu(\text{Zn–Cl})$, 268s $\nu(\text{Zn–Cl})$, 207s $\nu(\text{Zn–N})$, 195s $\nu(\text{Zn–N})$.
[B]	3448m $\nu(\text{O–H})$, 3177sh $\nu(\text{N–H})$, 3104vs $\nu(\text{C–H})$, 1628m $\nu(\text{C–C})$, 1605s $\nu(\text{C–N})$, 1593s, 1851s, 1495s, 1475s, 1456–1447vs [$\nu_{\text{s}}(\text{C–N})$, $\delta(\text{N–H})$, $\nu(\text{C–H})$], 1429vs, 1315vs, 1302s, 820s, 756vs $\delta(\text{C–H})$, 745vs $\delta(\text{C–H})$.	3068m $\nu(\text{C–H})$, 1629m $\nu(\text{C–C})$, 1601s $\nu(\text{C–N})$, 1582s, 1547vs, 1533vs, 1447vs [$\nu_{\text{s}}(\text{C–N})$, $\delta(\text{N–H})$, $\nu(\text{C–H})$], 1268vs [$\nu(\text{C–N})$, $\nu(\text{C–C})$], 1156s, 1013s, 974m, 628w, 582m, 531m, 330s, 315m $\nu(\text{Cd–Cl})$, 262s $\nu(\text{Cd–Cl})$, 205s $\nu(\text{Cd–N})$, 193s $\nu(\text{Cd–N})$.
[C]	3450m $\nu(\text{O–H})$, 3175sh $\nu(\text{N–H})$, 3108sb $\nu(\text{C–H})$, 1623sh $\nu(\text{C–C})$, 1601s $\nu(\text{C–N})$, 1593s, 1581s, 1495m, 1477s, 1454vs [$\nu_{\text{s}}(\text{C–N})$, $\delta(\text{N–H})$, $\nu(\text{C–H})$], 1443vs, 1429vs, 1315vs, 1300vs [$\nu(\text{C–N})$, $\nu(\text{C–C})$], 1233m, 993m, 820s, 743vs $\delta(\text{C–H})$, 678m, 663m 423s, 352m, 337m $\nu(\text{Hg–Cl})$, 276m $\nu(\text{Hg–Cl})$, 203s $\nu(\text{Hg–N})$, 179s $\nu(\text{Hg–N})$.	3069m $\nu(\text{C–H})$, 1627m $\nu(\text{C–C})$, 1600s $\nu(\text{C–N})$, 1581s, 1544vs, 1529vs, 1447vs [$\nu_{\text{s}}(\text{C–N})$, $\delta(\text{N–H})$, $\nu(\text{C–H})$], 1294m, 1267vs [$\nu(\text{C–N})$, $\nu(\text{C–C})$], 1154m, 1008vs, 972w, 807w, 740w $\delta(\text{C–H})$, 626w, 580m, 530m, 323s $\nu(\text{Hg–Cl})$, 266s $\nu(\text{Hg–Cl})$, 205s $\nu(\text{Hg–N})$, 192s $\nu(\text{Hg–N})$.
[D]	3415vs, 3237m, 3075m, 1642vs, 1618vs, 1608vs, 1477s, 1412s, 1365s, 1305s, 1147vs, 1118vs, 1109vs, 1083vs, 813s, 763s, 742, 629s, 432m.	3074m $\nu(\text{C–H})$, 1667m, 1605vs $\nu(\text{C–C})$, 1577vs $\nu(\text{C–N})$, 549, 430vs [$\nu_{\text{s}}(\text{C–N})$, $\delta(\text{N–H})$, $\nu(\text{C–H})$], 1304m, 1272s [$\nu(\text{C–N})$, $\nu(\text{C–C})$], 1148m, 1027s, 1010s, 582, 526m, 464s, 364m, 326m, 255m $\nu(\text{Fe–N})$, 204m $\nu(\text{Fe–N})$.

ν , Stretching; δ , bending; ω , wagging; m, medium; s, strong; w, weak; sh, shoulder; b, broad.

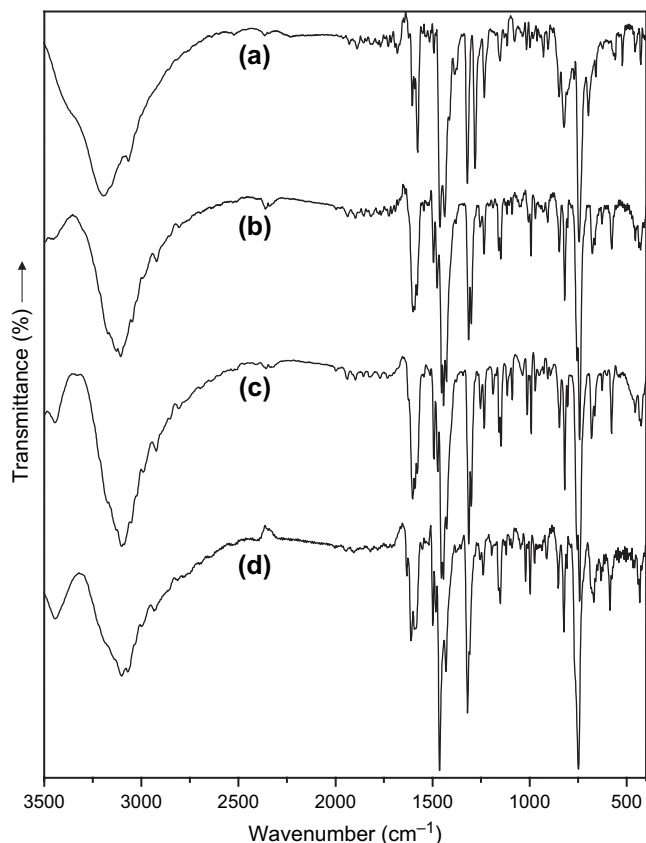


Fig. 3. FT-IR spectrum of (a) ligand, (b) $[\text{Hg}(\text{L})\text{Cl}_2]$, (c) $[\text{Cd}(\text{L})\text{Cl}_2]$, (d) $[\text{Zn}(\text{L})\text{Cl}_2]$ in the $3500\text{--}400\text{ cm}^{-1}$ region.

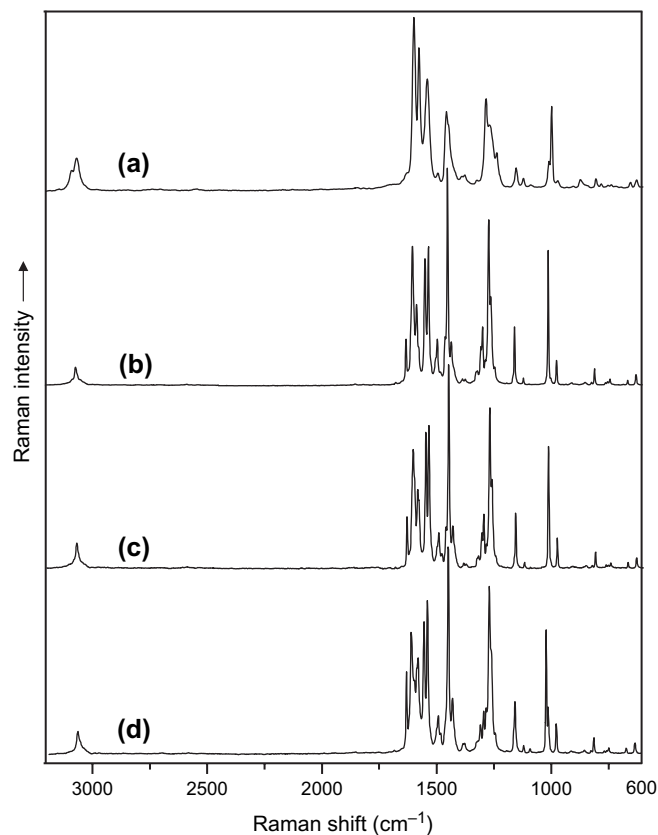


Fig. 4. Raman spectrum of (a) ligand, (b) $[\text{Hg}(\text{L})\text{Cl}_2]$, (c) $[\text{Cd}(\text{L})\text{Cl}_2]$, (d) $[\text{Zn}(\text{L})\text{Cl}_2]$ in the $3200\text{--}600\text{ cm}^{-1}$ region.

(Figs. 8 and 9). Complexation of metal ions with DNA bases is expected to bring about marked changes in its electronic spectrum. However, no marked changes have been observed in the electronic spectrum of these two complexes with the addition of DNA, ruling out the possibility of their direct coordinative binding to DNA donor atoms. With the addition of DNA, these two complex systems exhibit only small changes in their electronic spectrum. Such a small change may arise with groove binding, leading to small perturbations. This hyperchromism in the absorption intensity may probably be due to the dissociation of ligand aggregates [26] or due to its external contact (surface binding) with the duplex [27].

5.2. Microbial activity

The results concerning *in vitro* antimicrobial activities of the ligand, their hydrochloride salts, the metal salts and the complexes together with the inhibition zone (mm) and (MIC) values of compared antibiotic and antifungal activities are presented in Tables 4–6. All the compounds tested exhibit strong or moderate antimicrobial activity. Of all the test compounds attempted, $[\text{Zn}(\text{L})\text{Cl}_2]$ and $[\text{Hg}(\text{L})\text{Cl}_2]$ complexes showed the highest activities against most Gram positive and Gram negative bacteria and as well as yeast cultures. As an example, 25 (Hg), 21 (Zn), 29 (Hg), 26 (Zn) and 30 (Hg), 26 mm (Zn) inhibition zone values of the these complexes on

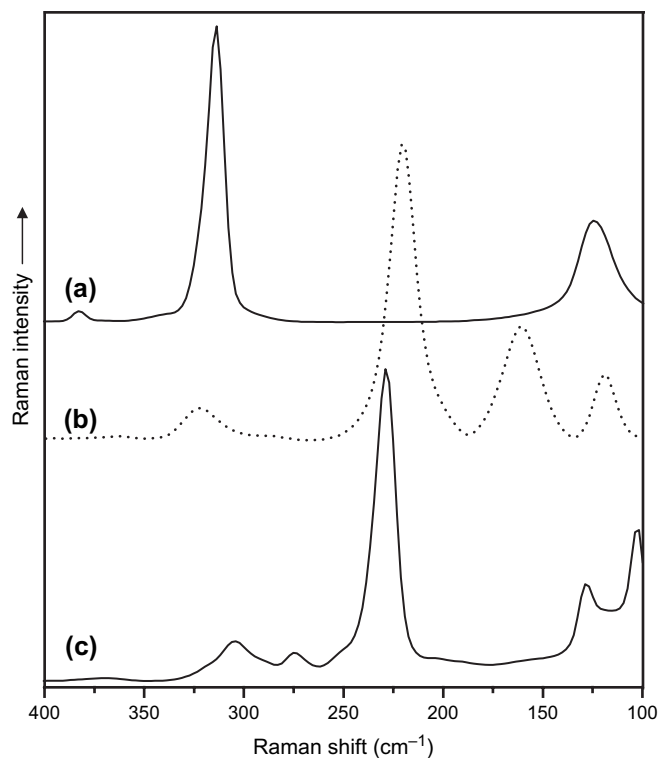


Fig. 5. Raman spectrum of (a) HgCl_2 , (b) CdCl_2 , (c) ZnCl_2 in the $400\text{--}100\text{ cm}^{-1}$ region.

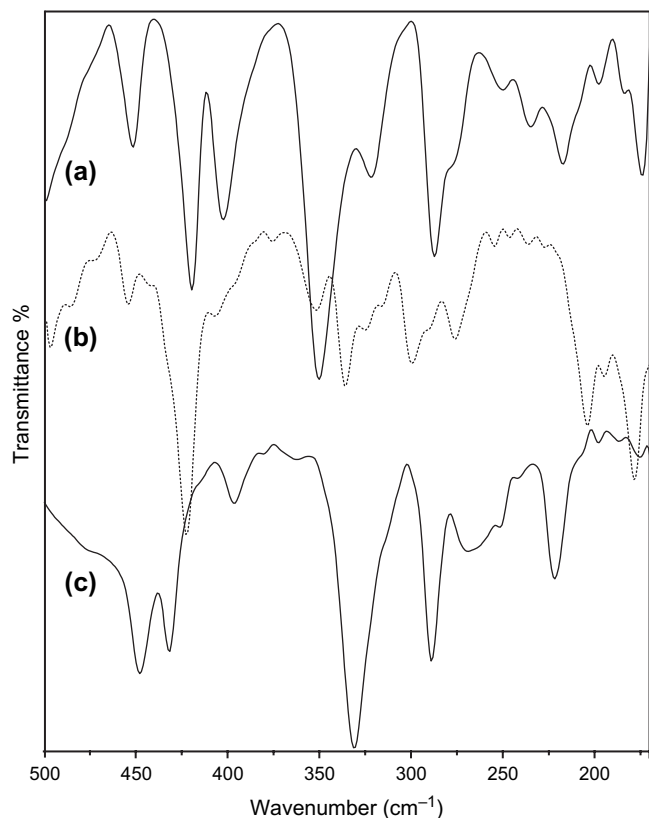


Fig. 6. The 500–175 cm^{-1} region FT-IR spectrum of (a) (L), (b) $[\text{Hg}(\text{L})\text{Cl}_2]$, (c) $[\text{Zn}(\text{L})\text{Cl}_2]$.

Escherichia coli (Gram negative), *Staphylococcus aureus* (Gram positive) and *Proteus vulgaris* (Gram negative) organisms are exceptionally effective compared with most of the reference antibiotics (Table 4). Similarly these two complexes show strong antifungal activity with the inhibition zone values of 27 (Hg), 24 (Zn) and 22 (Hg), 20 (Zn), 21 (Hg), 15 mm (Zn) inhibition on *Kluyveromyces fragilis*, *Candida albicans* and *Rhodotorula rubra* organisms, respectively (Table 5). These values are consistent and compatible with all the antifungal activities in comparison tests. The MIC values in Table 6 indicate that all the compounds tested exhibit moderate to strong antimicrobial activity on the tested microorganisms. Once again the microbial data indicate that the mercury and zinc complexes have a very strong and penetrating activity against most Gram positive and Gram negative bacteria and as well as yeast cultures. For instance, these two complexes showed superior activity against *S. aureus* (Gram positive) organism ($\text{MIC} = 0.78 \mu\text{g mL}^{-1}$) than the reference gentamycin ($\text{MIC} = 25 \mu\text{g mL}^{-1}$) or against *P. vulgaris* (Gram negative) organism ($\text{MIC} = 0.78$ (Hg), $1.56 \mu\text{g mL}^{-1}$ (Zn)) than the reference gentamycin ($\text{MIC} = 6.25 \mu\text{g mL}^{-1}$). Similarly the mercury and zinc complexes show improved antifungal activity compared to the other test compounds on most of the organisms, particularly against *K. fragilis* (0.78 (Hg), $1.56 \mu\text{g mL}^{-1}$ (Zn)) and *C. albicans* (3.125 (Hg), $3.125 \mu\text{g mL}^{-1}$ (Zn)) than the reference nystatin ($6.25 \mu\text{g mL}^{-1}$) and ($3.125 \mu\text{g mL}^{-1}$), respectively (Table 6). Surprisingly all of the test compounds attempted have either very weak or no effect under the given

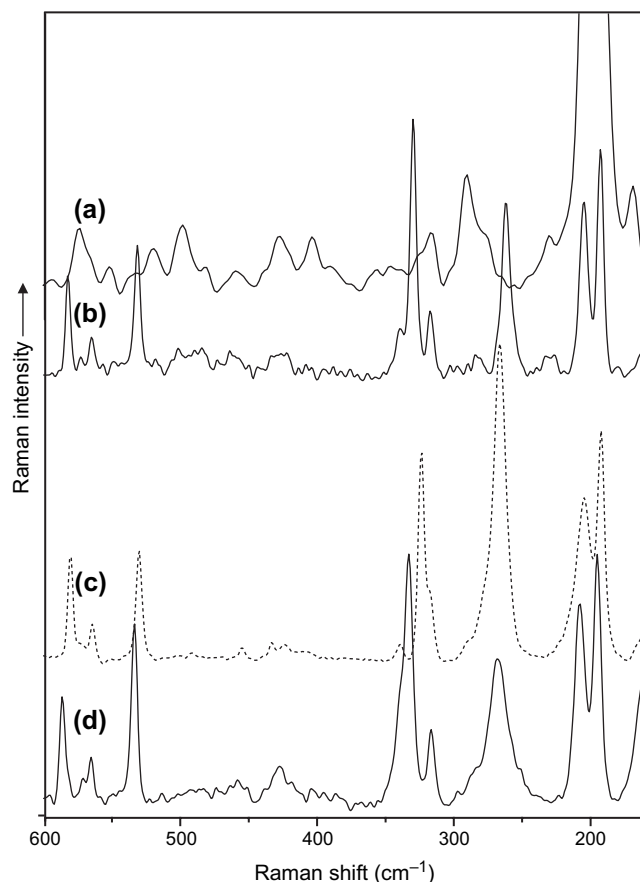


Fig. 7. Raman spectrum of (a) (L), (b) $[\text{Hg}(\text{L})\text{Cl}_2]$, (c) $[\text{Cd}(\text{L})\text{Cl}_2]$, (d) $[\text{Zn}(\text{L})\text{Cl}_2]$ in the 600–100 cm^{-1} region.

experimental conditions on *Mycobacterium smegmatis* and *Listeria monocytogenes* microorganisms.

The inhibition activity seems to be governed in certain degree by the facility of coordination at the metal centre, and therefore the complexes show stronger activity against the tested

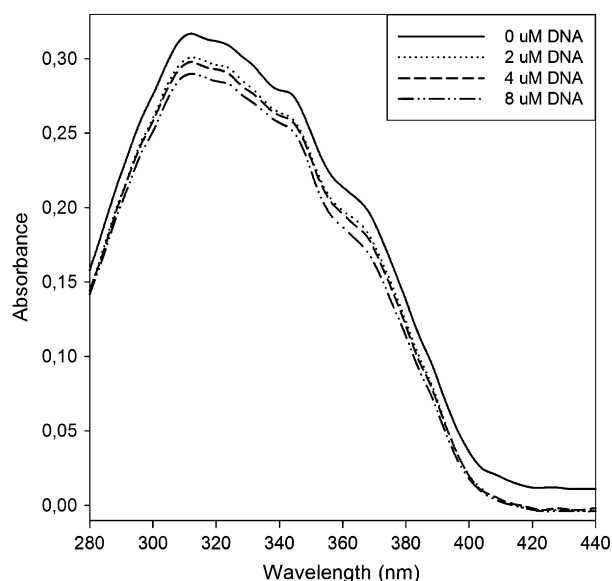


Fig. 8. UV-vis spectra of CT-DNA- $[\text{Zn}(\text{L})\text{Cl}_2]$ complex.

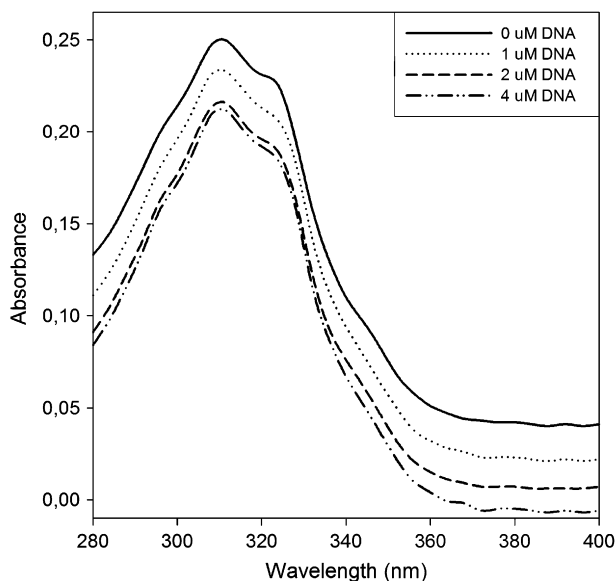


Fig. 9. UV-vis spectra of CT-DNA-[Hg(L)Cl₂] complex.

microorganisms, compared to the free ligands. This supports the argument that some type of bimolecular binding most probably occurs to the metal ions causing the inhibition of biological synthesis and preventing the organisms from reproducing.

In classifying the antibacterial activity as Gram positive or Gram negative, it would generally be expected that a much greater number would be active against Gram positive than Gram negative bacteria. However, in this study, the compounds are active against both types of the bacteria and as well as active against yeasts, which may indicate broad-spectrum properties.

The results of our study indicate that the complexes as a whole, but particularly essential zinc complex, have the potential to generate novel metabolites, by displaying moderate to high affinities for most of the receptors. This compound could be selected for further pharmacological tests to be evaluated as potential drug against many infectious diseases.

6. Experimental

6.1. Chemistry

Apart from *o*-phenylenediamine (freshly sublimed), all other chemicals and solvents were used as commercial

products of analytical grade without any purification. Molar conductivity of the complexes was measured on a WPA CMD750 conductivity meter in dimethyl sulfoxide (DMSO) solution at 25 °C. UV-vis spectral measurements of the complexes, and DNA binding studies were carried out on Unicam Alpha Helios spectrophotometer at 25 °C. FT-IR spectra were recorded in KBr pellets (mid, 4000–400 cm⁻¹) and in polyethylene discs (far, 600–170 cm⁻¹) on a Jasco FT/IR-600 Plus Spectrometer. Raman spectra were obtained from powdered samples placed in a Pyrex tube using a Bruker RFS 100/S Raman spectrometer in the range 4000–0 cm⁻¹. The 1064 nm line, provided by a near infrared Nd:YAG air-cooled laser was used as excitation line. The output laser power was set to 100–120 mW. Routine ¹H and ¹³C NMR spectra were recorded at ambient temperature on a 500 MHz NMR Spectrometer in DMSO-*d*₆. Chemical shifts (δ) are expressed in units of part per million relative to tetramethylsilane.

6.1.1. Synthesis

6.1.1.1. 2,6-Bis(benzimidazol-2-yl)pyridine ligand (L). The ligand (L) was prepared according to the literature procedures [5,17], by reacting a mixture of pyridine-2,6-dicarboxylic acid (3.34 g, 20 mmol) and freshly sublimed *o*-phenylenediamine (4.32 g, 40 mmol) in 5 M HCl (40 mL) at reflux temperature. The precipitates were collected and neutralized by aqueous ammonia.

6.1.1.2. [Zn(L)Cl₂] complex [A]. Hot solution mixture of (L) (156 mg, 50 mmol) and ZnCl₂ (75 mg, 55 mmol) in EtOH (10 mL) was reacted for several hours. The pale-yellow solid products were collected, washed with small portions of EtOH and dried in vacuum.

6.1.1.3. [Cd(L)Cl₂] complex [B] [15]. Complex [B] was synthesized in a similar manner to that used for complex [A], reacting a mixture of (L) (156 mg, 50 mmol) and CdCl₂ (100 mg, 55 mmol) in EtOH (10 mL).

6.1.1.4. [Hg(L)Cl₂] complex [C]. Complex [C] was synthesized in a similar manner to that used for complex [A],

Table 4

In vitro antibacterial activities of compounds and standard reagents (inhibition zone, mm)

Microorganisms	(1)	(2)	(3)	(4)	(5)	(6)	(7)	(8)	(9)	(10)	PEN	SAM	CTX	VAN	OFL	TET
<i>Escherichia coli</i>	14	16	13	12	14	14	16	18	21	25	18	12	10	22	30	28
<i>Staphylococcus aureus</i>	15	13	16	11	15	18	21	24	26	29	13	16	12	13	24	26
<i>Klebsiella pneumoniae</i>	8	10	9	8	12	12	12	14	14	15	18	14	13	22	28	30
<i>Bacillus cereus</i>	11	10	9	12	10	12	11	14	15	15	14	12	14	18	30	25
<i>Micrococcus luteus</i>	12	14	12	14	13	15	16	18	16	20	36	32	32	34	28	22
<i>Proteus vulgaris</i>	11	14	10	12	14	17	21	24	26	30	10	16	18	20	28	26
<i>Mycobacterium smegmatis</i>	8	9	8	8	10	11	11	10	12	12	15	21	11	20	32	24
<i>Listeria monocytogenes</i>	10	9	8	10	11	12	10	12	12	12	10	12	16	26	30	28
<i>Pseudomonas aeruginosa</i>	10	12	11	12	11	12	11	13	14	16	8	10	54	10	44	34

PEN, penicillin G; SAM, ampicillin; CTX, cefotaxime; VAN, vancomycin; OFL, ofloxacin; TET, tetracyclin; (1), (ZnCl₂); (2), (HgCl₂); (3), (CdCl₂); (4), [Fe(ClO₄)₂]; (5), (L); (6), [(L)(3HCl)]; (7), [Fe(ClO₄)₂(L)]; (8), [CdCl₂(L)]; (9), [ZnCl₂(L)]; (10), [HgCl₂(L)].

Table 5
In vitro antifungal activities of compounds and standard reagents (inhibition zone, mm)

Microorganisms	(1)	(2)	(3)	(4)	(5)	(6)	NY	KET	CLT
<i>Candida albicans</i>	14	15	15	17	20	22	20	21	15
<i>Kluyveromyces fragilis</i>	15	18	21	20	24	27	18	16	18
<i>Rhodotorula rubra</i>	12	14	14	18	15	21	18	22	16
<i>H. guilliermondii</i>	12	14	12	14	15	18	21	24	22
<i>Debaryomyces hansenii</i>	11	13	12	14	15	17	16	14	18

NY, nystatin; KET, ketaconazole; CLT, clotrimazole; (1), (L); (2), [(L)(HCl)₃]; (3), [Fe(ClO₄)₂(L)]; (4), [CdCl₂(L)]; (5), [ZnCl₂(L)]; (6), [HgCl₂(L)].

reacting a mixture of (L) (125 mg, 40 mmol) and HgCl₂ (120 mg, 44 mmol) in EtOH (10 mL).

6.1.1.5. [Fe(L)₂](ClO₄)₂ complex [D] [16]. Complex [D] was prepared in a similar manner to that used for complex [A], reacting a mixture of (L) (125 mg, 40 mmol) and Fe(ClO₄)₂ (112 mg, 44 mmol) in EtOH (8 mL).

6.2. Pharmacology

6.2.1. Microorganisms

The antimicrobial activities are evaluated against Gram positive (*S. aureus*, *Bacillus cereus*, *M. smegmatis*, *L. monocytogenes*, *Micrococcus luteus*) and Gram negative (*E. coli*, *Klebsiella pneumoniae*, *Pseudomonas aeruginosa*, *P. vulgaris*, *Enterobacter aerogenes*) bacteria and the yeast cultures (*C. albicans*, *K. fragilis*, *R. rubra*, *D. hansenii* and *H. guilliermondii*) using disk diffusion method as well as the minimal inhibitory concentration (MIC) dilution method which are outlined in Section 6.

6.2.2. Antimicrobial screening

6.2.2.1. *Disk diffusion method.* Sterilized antibiotic discs (6 mm) were used following the literature procedure [28,29]. Fresh stock solutions (30 μg mL⁻¹) of the ligand and the complexes were prepared in redistilled dimethyl sulfoxide

Table 6
In vitro antimicrobial activity of compounds and standard reagents (MIC, μg mL⁻¹)

Microorganisms	(1)	(2)	(3)	(4)	(5)	(6)	(7)	(8)	(9)	(10)	GN	NY
<i>Escherichia coli</i>	12.5	6.25	12.5	25	12.5	12.5	6.25	3.125	3.125	1.56	6.25	–
<i>Staphylococcus aureus</i>	6.25	12.5	6.25	25	12.5	3.125	1.56	1.56	0.78	0.78	25	–
<i>Klebsiella pneumoniae</i>	100	50	50	50	50	50	50	25	12.5	12.5	6.25	–
<i>Bacillus cereus</i>	25	25	50	50	100	50	50	25	12.5	12.5	6.25	–
<i>Micrococcus luteus</i>	12.5	12.5	12.5	12.5	12.5	12.5	6.25	6.25	6.25	3.125	25	–
<i>Proteus vulgaris</i>	25	12.5	25	12.5	12.5	6.25	3.125	1.56	1.56	0.78	6.25	–
<i>Mycobacterium smegmatis</i>	100	50	100	50	100	100	50	100	50	50	12.5	–
<i>Listeria monocytogenes</i>	25	50	50	25	100	50	100	50	50	50	12.5	–
<i>Pseudomonas aeruginosa</i>	25	14.5	25	12.5	100	100	100	50	12.5	6.25	6.25	–
<i>Kluyveromyces fragilis</i>	12.5	12.5	12.5	12.5	12.5	3.125	3.125	3.125	1.56	0.78	–	6.25
<i>Rhodotorula rubra</i>	50	25	50	12.5	50	12.5	12.5	3.125	12.5	3.125	–	6.25
<i>Candida albicans</i>	12.5	12.5	12.5	12.5	12.5	12.5	12.5	6.25	3.125	3.125	–	3.125
<i>H. guilliermondii</i>	12.5	50	25	25	50	50	50	12.5	12.5	6.25	–	3.125
<i>Debaryomyces hansenii</i>	50	25	25	25	50	50	50	12.5	12.5	6.25	–	12.5

GN, gentamycin; NY, nystatin; (1), (ZnCl₂); (2), (HgCl₂); (3), (CdCl₂); (4), [(Fe(ClO₄)₂); (5), (L); (6), [(L)(3HCl)]; (7), [Fe(ClO₄)₂(L)]; (8), [CdCl₂(L)]; (9), [ZnCl₂(L)]; (10), [HgCl₂(L)].

(DMSO) according to the required concentrations (compounds are not soluble in water). To ensure that the solvent had no effect on bacterial growth, a control test was performed with test medium supplemented with DMSO as the same procedures as used in the experiments. The discs were impregnated with 20 μL of these solutions. All the bacteria were incubated and activated at 30 °C for 24 h inoculation into nutrient broth, and the yeasts were incubated in malt extract broth for 48 h. Inoculums containing 10⁶ bacterial cells or 10⁸ yeast cells per mL were spread on Mueller–Hinton Agar plates (1 mL inoculum for each plate). The discs injected with solutions were placed on the inoculated agar by pressing slightly and incubated at 35 °C (24 h) and at 25 °C (72 h) for bacteria and yeast, respectively. On each plate an appropriate reference antibiotic disc was applied depending on the test microorganisms. In each case triplicate tests were performed and the average was taken as the final reading.

6.2.2.2. *Dilution method.* Screening was performed following the procedure outlined in the Manual of Clinical Microbiology [6,30]. All the bacteria were incubated and activated at 30 °C for 24 h inoculation into nutrient broth and the yeasts were incubated in malt extract broth for 48 h. The compounds were dissolved in DMSO and then diluted using cautiously adjusted Mueller–Hinton broth. Two-fold serial concentrations of the compounds were employed to determine the (MIC) ranging from 100 μg mL⁻¹ to 0.78 μg mL⁻¹. In each case triplicate tests were performed and the average was taken as the final reading.

Cultures are grown at 37 °C (20 h) and the final inoculation (inoculums) was approximately 10⁶ cfu mL⁻¹. Test cultures are incubated at 37 °C (24 h). The lowest concentrations of antimicrobial agents that result in complete inhibition of microorganisms are represented as (MIC) μg mL⁻¹. In each case triplicate tests were performed and the average was taken as the final reading.

6.2.2.3. *DNA binding.* Calf thymus DNA was purchased from Worthington Biochemical Corp. and dissolved in 10 mM

Tris–HCl buffer at pH 8.0. CT-DNA in the buffer gave a ratio of UV absorbance at 260 and 280 nm of 1.9:1, indicating that DNA was free from protein [31]. The DNA concentration per base pair was determined by absorption spectroscopy using the molar absorption coefficient ($12824 \text{ M}^{-1} \text{ cm}^{-1}$) [32]. The absorption spectra of the complex [10 μM in buffer–DMSO (1:1 v/v)] was obtained in the absence and presence of increasing amounts of CT-DNA ([DNA] = 0–10 μM).

References

- [1] R. Canetta, M. Rozenzweig, R.E. Wittes, L.P. Schacter, *Cancer Chemotherapy: Challenges for the Future*, vol. 5, Excerpta Medica, Tokyo, 1990, p. 318.
- [2] B. Rosenberg, B. Lippert, *Cisplatin, Chemistry and Biochemistry of a Leading Anticancer Drug*, Verlag Chemie VCH, Basel, 1999, p. 3.
- [3] I.H. Krakoff, M. Nicali (Eds.), *Platinum and Other Metal Coordination Compounds in Cancer Chemotherapy: Clinical Application of Platinum Complexes*, Martinus Nijhoff, Boston, 1988, p. 351.
- [4] K.K. Monthilal, C. Karunakaran, A. Rajendran, R. Murugesan, *J. Inorg. Biochem.* 98 (2004) 322.
- [5] M. NazAgh-Atabay, B. Dulger, F. Gucin, *Eur. J. Med. Chem.* 38 (2003) 875.
- [6] M. NazAgh-Atabay, B. Dulger, F. Gucin, *Eur. J. Med. Chem.* 40 (2005) 1096.
- [7] F.J. Schendel, Y.S. Cheng, J.D. Otvos, S. Vehrli, J. Stubbe, *Biochemistry* 27 (1988) 2614.
- [8] R.V. Devivar, E. Kawashima, G.R. Revankar, J.M. Breitenbach, E.D. Kreske, J.C. Drach, L.B. Townsend, *J. Med. Chem.* 37 (1994) 2942.
- [9] L.B. Townsend, R.V. Devivar, S.R. Turk, M.R. Nassiri, J.C. Drach, *J. Med. Chem.* 38 (1995) 4098.
- [10] H. Irving, P.J.R. Williams, *J. Chem. Soc.* (1953) 3192.
- [11] (a) R.G. Pearson, *J. Am. Chem. Soc.* 85 (1963) 3353;
(b) R.G. Parr, R.G. Pearson, *J. Am. Chem. Soc.* 105 (1983) 7512.
- [12] V. Ganesan Vaidyanathan, B. Unni Nair, *J. Inorg. Biochem.* 91 (2002) 405.
- [13] S.J. Lippard, J.M. Berg, *Principles of Bioinorganic Chemistry*, University Science Books, Mill Valley, CA, 1994, pp. 103–137.
- [14] R. Boca, P. Baran, L'ubor Dlhán, H. Fuess, W. Haase, F. Renz, W. Linert, I. Svoboda, R. Werner, *Inorg. Chim. Acta* 260 (1997) 129.
- [15] Sheng-Gui Liu, Jing-Lin Zuo, Yi-Zhi Li, Xiao-Zeng You, *J. Mol. Struct.* 705 (2004) 153.
- [16] M. Hasegawaa, F. Renzb, T. Haraa, Y. Kikuchia, Y. Fukudab, J. Okuboc, T. Hoshia, W. Linertd, *Chem. Phys.* 277 (2002) 21.
- [17] A.W. Addison, P.J. Burke, *Heterocycl. Chem.* 18 (1981) 803.
- [18] A.D. Becke, *Phys. Rev. A* 38 (1988) 3098.
- [19] J. Perdew, *Phys. Rev. B* 33 (1986) 8822.
- [19] J. Perdew, *Phys. Rev. B* 34 (1986) 7046.
- [20] R.N. Mohanty, V. Chakravorty, K.C. Dash, *Polyhedron* 10 (1991) 33.
- [21] A. Gelling, K.G. Orrell, A.G. Osborne, V. Sik, M.B. Hursthouse, D.E. Hibbs, K.M.A. Malik, *Polyhedron* 13–14 (1998) 2141.
- [22] K. Nakamoto, *Infrared, Raman Spectra of Inorganic Coordination Compounds, Part B, fifth ed.* 1997, pp. 23–33.
- [23] D.A. Thornton, *Coord. Chem. Rev.* 104 (1990) 251.
- [24] D. Demertzi, D. Nicholls, *Inorg. Chim. Acta* (1983) 73.
- [25] S. Akyüz, J.E.D. Davis, A.B. Dempster, K.T. Holmes, *J. Chem. Soc. Dalton. Trans.* (1976) 1746.
- [26] Rajamanickam Vijayalakshmi, Mookandi Kanthimathi, Venkatesan Subramanian, Balachandran Unni Nai, *Biochim. Biophys. Acta* 1475 (2000) 157.
- [27] R. Tamilarasan, D.R. McMillin, *Inorg. Chem.* 29 (1990) 2798.
- [28] *Performance Standards for Antimicrobial Disk Susceptibility Tests, Approved Standard NCCLS Publication M2-A5*, Villanova, PA, USA, 1993, pp. 1–32.
- [29] C.H. Collins, P.M. Lyre, J.M. Grange, *Microbiological Methods*, sixth ed. Butterworths Co. Ltd., London, 1989.
- [30] R.N. Jones, A.L. Barry, T.L. Gaven, J.A. Washington, in: E.H. Lennette, A. Balows, W.J. Shadomy (Eds.), *Manual of Clinical Microbiology*, fourth ed. American Society for Microbiology, Washington DC, 1984, pp. 972–977.
- [31] J. Marmur, *J. Mol. Biol.* 3 (1961) 208.
- [32] D. Suh, J.B. Chanes, *Bioorg. Med. Chem.* 3 (1995) 723.